Crack Growth Monitoring by Embedded Optical Fibre Bragg Grating Sensors

Fibre Reinforced Plastic Crack Growing Detection

G. Pereira, L. Mikkelsen and M. McGugan

Technical University of Denmark, Department of Wind Energy, Frederiksborgvej 399, 4000 Roskilde, Denmark

Keywords: Fibre Bragg Grating Sensors, Crack Growth Monitoring, Fibre Reinforced Plastic Crack Monitoring, Digital Image Correlation.

Abstract: This article presents a novel method to asses a crack growing/damage event in fibre reinforced plastic, or adhesive using Fibre Bragg Grating (FBG) sensors embedded in a host material. Different features of the crack mechanism that induce a change in the FBG response were identified. Double Cantilever Beams specimens made with glass fibre glued with structural adhesive, were instrumented with an array of FBG sensors embedded in the material and tested using an experimental fracture procedure. A digital image correlation technique was used to determine the presence of the specific phenomena caused by the crack, and to correlate with the FBG sensor. A Material-Sensor model was developed in order to predict the sensor output response under a crack/delamination situation, which can be used as an analysis tool for future application of this measurement technology in more complex structures.

1 INTRODUCTION

1.1 Fibre Reinforced Plastic Materials

Fibre reinforced plastic (FRP) materials (composite materials) have been extensively used in aerospace, automotive, naval, civil engineering and wind energy applications. These fibre reinforced materials consist of two macroscopic phases, a stiff fibre phase (usually glass or carbon fibre) and a polymer matrix (usually polyester or epoxy). The main advantage of this material is its capability to be tailored for a specific application, this enables an enhancement, and a high level of customization of mechanical properties, such as light-weight, thermal expansion, chemical/corrosion resistance, fatigue behaviour, etc (Jones, 1999).

The increased used of fibre reinforced plastic materials requires a proper understanding of the failure mechanisms. Delamination is one of the most important failure mechanisms and is considered the most widespread mode of life reduction.

1.2 Delamination/Damage Mechanism

Often in fibre reinforced polymers, delamination is accompanied by the formation of a crack bridging zone, where intact fibres connect the crack faces behind the crack tip, thus the energy required for the crack to propagate is higher that required to initiate. The relationships between the crack bridging stresses and the crack opening displacement (bridging laws) are used to describe the effect of fibres on the crack propagation (B.F. Sørensen, 2010). The cracking in homogeneous isotropic materials usually occurs under pure Mode I (opening loading) but in weak planes or along interfaces, like in composite materials cracking, occurs under a combination of Modes (Shear and opening loading). Figure 1 shows the *fibre bridging phenomenon* in a fibre reinforced polymer specimen.

Figure 1: Fibre bridging phenomenon in a fibre reinforced polymer specimen.

Another important feature of the fibre bridging phenomena for our study case, is the formation of a compression field ahead the crack tip, and traction before the crack tip. The fibres connecting the crack

Pereira G., Mikkelsen L. and McGugan M..
Crack Growth Monitoring by Embedded Optical Fibre Bragg Grating Sensors - Fibre Reinforced Plastic Crack Growing Detection.
DOI: 10.5220/0005325901330139
In *Proceedings of the 3rd International Conference on Photonics, Optics and Laser Technology* (OSENS-2015), pages 133-139
ISBN: 978-989-758-092-5

faces behind the crack tip will act like cables, forcing the faces to close, creating a traction stress in that area. However, to maintain a force equilibrium, a compression field is formed ahead the crack tip. The compression-traction fields move as the crack grows.

1.3 Crack/Delamination Detection in Fibre Reinforced Plastic Materials

Sensing technology has been implemented in order to track delamination in FRP materials. Acoustic emission (Silversides et al., 2013) that measures the stress waves generated by the crack front growing, vibration (Kyriazoglou and Guild, 2004) that detects changes in the specific damping capacity of the structure, model analysis (Hu et al., 2006) by monitoring the material natural frequencies and mode shapes, piezo-electric actuators/sensors and wavelet analysis (Yan and Yam, 2002) based on the energy variation of the structural dynamic. However, these measurement systems have several limitations, among these the need for qualified operators, expensive hardware and impractical to use under operation. Also, to detect delamination in FRP materials the sensor must be embedded in the laminate layers or in the interface of the FRP and a structural adhesive.

Fibre Bragg Gratings (FBG) have the capability to be embedded in the FRP material, even in an operational structure, without compromising its structural resistance. This is due to the FBG reduced size, with a diameter of $125\,\mu m$, it is virtual non-intrusive to the material. Also, FBG sensors present other interesting features, such high resolution, multiplexing capability, immunity to electromagnetic fields, chemical inertness and long term stability (fatigue behaviour).

1.4 Crack/Delamination Detection by Embedded Fibre Bragg Gratings

During a crack/delamination event different fracture features will be present near the crack tip. Being able to identify and measure this specific phenomena with a FBG sensor is a key factor to correctly determine the presence of damage and it growth.

In figure 2, the different stages of the FBG responses under a crack growth event are presented. First, before the crack reach the proximity of the grating, figure 2a), the material will build up uniform strain (considering structure loading or geometric singularities distant enough from the grating), that will make a uniform wavelength shift in the FBG reflected peak. Next, a compression field is formed ahead of the crack tip due to the formation of a crack bridging zone, witch was discussed in section 1.2, will reach the grating area creating a peak splitting of the FGB response, figure 2b). This peak split phenomena will be discussed later, but briefly is due a birefringent effect. Then, when the grating is near the influence of the crack singularity (region dominated by stress concentration) a non-uniform strain field will also create a change in the shape of the reflected peak, as showed in figure 2c). Finally, after the crack passes the FBG sensor, the shape of the reflected peak will go back to the original shape, and the sensor response will again be a simple wavelength shift, because at this stage only uniform strains will be present in the FBG proximity, figure 2d).

2 FIBRE BRAGG GRATING WORKING PRINCIPLE

A Fibre Bragg Grating (FBG) is formed by a permanent periodic modulation of the refractive index along a section of an optical fibre, by exposing the optical fibre to an interference pattern of intense ultra-violet light (Hill and Meltz, 1997). The photosensitivity of the silica exposed to the ultra-violet light is increased, so when the optical fibre is illuminated by a broadband light source a very narrow wavelength band is reflected back. The spectral response of a homogeneous FBG is a single peak centred at the wavelength λ_b. The wavelength λ_b is described by the Bragg condition ,

$$\lambda_B = 2n_{eff,0}\Lambda_{,0} \quad (1)$$

where n_0 is the mean effective refractive index at the location of the grating, the index 0 denotes unstrained conditions (initial state). n_{eff} is the effective refractive index and Λ is the constant nominal period of the refractive index modulation (Morey et al., 1990).

2.1 Fibre Bragg Grating Response to a Uniform Variation of Strain and/or Temperature

The wavelength shift $\Delta\lambda_b$ of an embedded FBG under a uniform variation of strain ε_{zz}, and temperature ΔT is given by the equation 2 (Zhang et al., 2008),

$$\frac{\Delta\lambda_b}{\lambda_b} = (1-p_e)\varepsilon_{zz} + [(1-p_e)(\alpha_s-\alpha_f)+\xi]\Delta T \quad (2)$$

where p_e is a photoelastic coefficients, α_s and α_f are the thermal expansion coefficients of the host material and the optical fibre, respectively, and ξ is the thermo-optic coefficient.

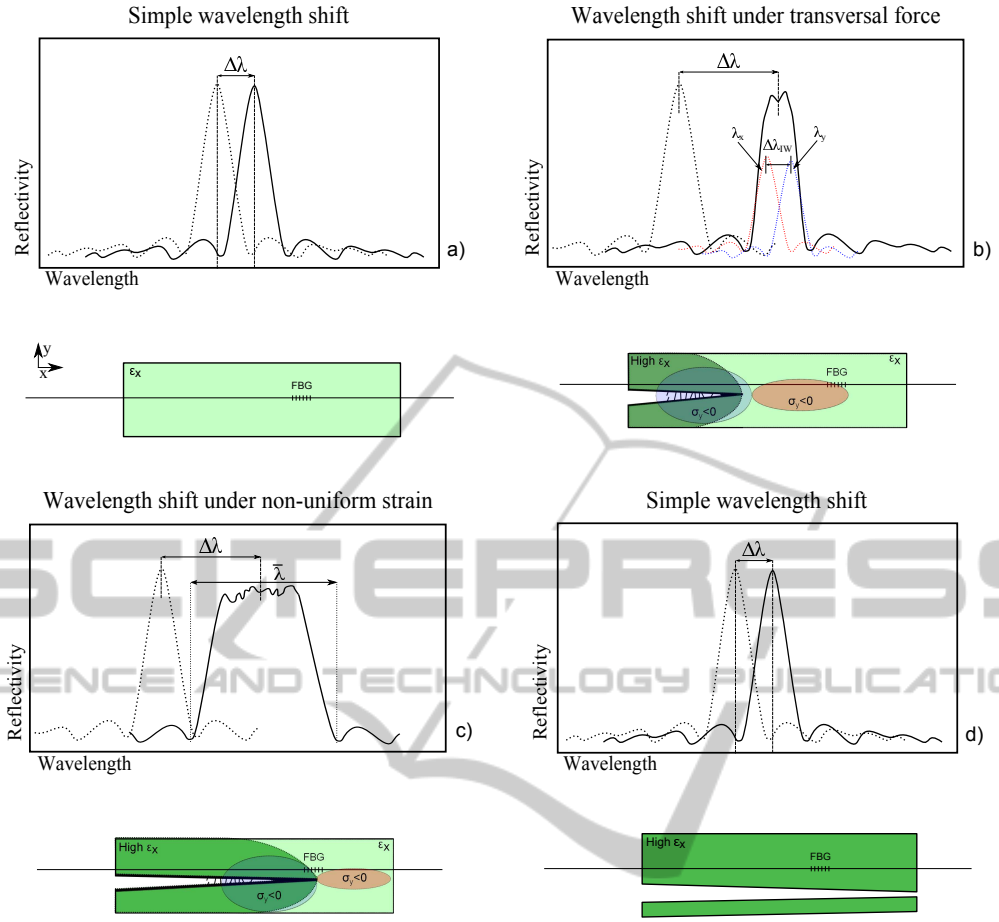

Figure 2: Different stages of the FBG responses under a crack growth event.

2.2 Fibre Bragg Grating Response Under a Transverse Force: Birefringent Effect

An optical fibre can present a birefringent behaviour, defined by the change of the refractive index n_{eff} in the two directions n_{effx} and n_{effy}, when the grating is subjected to a transverse force. The variation of the refractive index in the two directions n_{effx} and n_{effy} is given by the equation (3) and (4) (Sørensen et al., 2007; Zhang et al., 2014; Jülich and Roths, 2010; Bosia et al., 2003).

$$\Delta n_x = -\frac{n_0^3}{2E_f}\{(p_{11}-2\nu_f p_{12})\sigma_x + [(1-\nu_f)p_{12}-\nu_f p_{11}](\sigma_y+\sigma_z)\} \quad (3)$$

$$\Delta n_y = -\frac{n_0^3}{2E_f}\{(p_{11}-2\nu_f p_{12})\sigma_y + [(1-\nu_f)p_{12}-\nu_f p_{11}](\sigma_x+\sigma_z)\} \quad (4)$$

$\sigma_{y,x}$ is the transverse stress, E_f is the elastic modulus of the optical fibre,ν_f is the Poisson's ration, n_0 is the initial refractive index, p_{11} and p_{12} are the photo-elastic coefficients of the optical fibre.

Rewriting the equation (3) and (4) it is possible to determine the increase in the width of the reflected peak, $\Delta\lambda_{IW} = \|\lambda_x - \lambda_y\|$, caused only by a transverse stress.

$$\begin{aligned}\Delta\lambda_{IW} &= 2\Lambda\|\Delta n_{effx} - \Delta n_{effx}\| \\ &= \frac{\Lambda n_o^3}{E_f}[(1+\nu_f)p_{12}-(1+\nu_f)p_{11}]\|\sigma_y\|\end{aligned} \quad (5)$$

2.3 Fibre Bragg Grating Response Under a Non-uniform Strain

When an FBG sensor is near a defect, a crack, a material change or a geometric variation, this can create a stress concentration that will lead to an abrupt variation of strain. This non-uniform strain will change

the periodicity of the grating pattern along the sensor length, modifying the grating pattern configuration from "uniform" to "chirped" (Yashiro et al., 2007; Zhang et al., 2007).

As demonstrated by Peters (Peters et al.,), in a uniform grating the applied strain will induce a change in both grating period and the mean index. These two effects can be superimposed by applying an effective strain of "$(1-p_e)\varepsilon_{zz}(z)$", similar the first part of equation (2) but taking into account the strain variation along the z direction. Then it is possible to rewrite the grating period as:

$$\Lambda(z) = \Lambda_0[1 + (1-pe) \times \varepsilon_{zz}(z)] \quad (6)$$

Where Λ_0 is the grating period with zero strain. The non-uniform strain effect can be approximated by using the maximum and minimum strain values along the grating. So, the maximum grating period Λ_{max} and minimum Λ_{min} can be calculated using the equation (6). Thus, an approximated increase of the width of the reflected peak due to a non-uniform strain $\Delta\lambda_{IW}$ is given by combining equations (6) and (1),

$$\Delta\lambda_{IW} = 2n_{eff}\Lambda_{max} - 2n_{eff}\Lambda_{min} \quad (7)$$

3 MATERIAL AND EXPERIMENTAL PROCEDURE

In order to measure the different features of the fracture mechanism, experiments were conducted on Double Cantilever Beams (DCB) with embedded FBG sensors, subjected to a fracture testing procedure.

3.1 Material and Testing Procedure

Eight (8) DCB specimens were tested in a loading device commonly used to determine material fracture properties, developed by (Sørensen et al., 2006). The DCB specimens were loaded in different conditions at 1 mm/min, ranging pure Mode I to pure Mode II, in order to simulate the different crack/delamination situations. Using this testing technique allows stable crack growth and makes it possible to correctly evaluate the FBG response at different stages.

The DCB specimens were manufactured using two composite material arms, made of a mix of unidirectional and triaxial glass layers (SAERTEX UD and TRIAX), that were glued by a commercial epoxy structural adhesive (Epikote MGS BPR 135G/Epikote MGS BPH137G). The geometry of the DCB specimen is presented in figure 3.

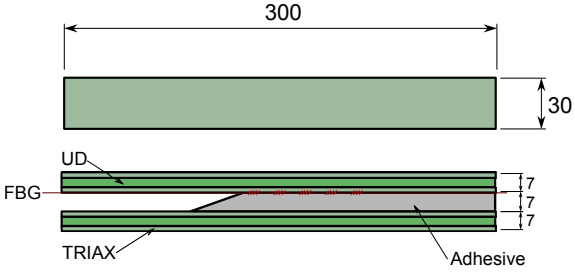

Figure 3: Sketch of the specimen geometry.

3.2 Sensors and Measurement Technology

An array of 5 uncoated single mode (SM) FBG sensors, witch with a length of *10 mm*, were embedded in the interface of the composite material with the structural adhesive. The gratings array were spaced by *10 mm* from each other, and the first grating was positioned 10 mm from the edge of the adhesive. The sensors were connected to a Optical Spectral Analyser (OSA) *FS2200 - Industrial BraggMETER* from FiberSensing™.

A digital image correlation technique was applied to the specimens, in order to determine the presence of specific phenomenon caused by the crack (ex:non-uniform strain) and to correlate it with the FBG output. Digital image correlation is an optical method that by tracking changes in a random pattern in the specimen, can correlate this information with deformation/strain in the material. A pattern was painted on the side surface of the DCB specimen and ARAMIS™software was used to calculated the strains from each measurement.

All the measurements from the Braggmeter and Aramis were synchronized with the crack growth.

4 DISCUSSION OF RESULTS

Figure 4 shows some measurements from a five (5) FBG array embedded in a DCB under a Mode II fracture testing (the full test was more measurement points, but is not possible to show it all in this article). The reflected peak at 1580 nm (furthest to the right) corresponds to the grating closest to the crack tip, and consequently the peak at 1530 nm (furthest to the left)is the most distant. It is possible to observe changes in the reflected peaks as the crack propagates. This change in the shape of the reflected peaks is due the proximity of the crack, as described in section 1.4. Evaluating and tracking this change will permit a determination of the presence and position of the crack.

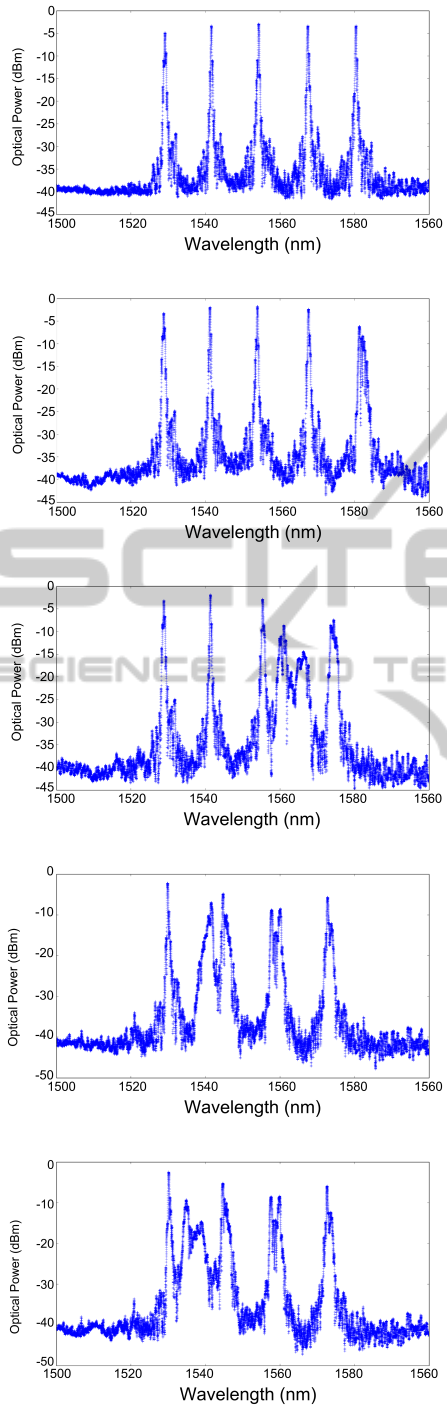

Figure 4: FBG array output under Mode II crack growing.

Figure 5 presents the shape of the reflected peak (FBG 5- 1580nm) during a crack growth under Mode II. Digital image correlation technique was used in order to determine the strain/stress shape distribution during the measurement.It shows the different crack features that can change the shape of the reflected peak, as described in section 1.4 and figure 2. The measurement pictures in the left column (ε_y compression) presents the specimen areas with compression stress (blue area). These compression areas can cause the birefringent effect in the FBG sensor, as described in 2.2. The measurement pictures in the center column (ε_x- Non-uniform), present the longitudinal strain in the specimen, where a gradient of colors represent variation of strain. This non-uniformity of strain can also create a change in the shape of the reflected peak, as described in 2.3.

As described in section 1.4, it is possible to identify the different stages of the crack growth from the sensor response. Before the crack reach the proximity of the grating, the material builds up uniform strain, that induces a uniform wavelength shift in the sensor response. Next, the compression field that was formed ahead of the crack tip reaches the grating area creating a peak splitting/increase of the width. Then, when the grating is near the influence of the crack singularity (region dominated by stress concentration), the non-uniform strain field creates a change in the shape of the reflected peak. Finally, after the crack passes the FBG sensor the shape of the reflected peak is gradually recovered to the original shape.

5 CONCLUSIONS

In this article the capability of Fibre Bragg Gratings embedded in composite material to detect and track cracks/delamination was demonstrated. The use of digital image correlation technique proved that specific fracture features near the crack can create a change in the shape of the reflected peak. Thus, it is possible to extract information from sensor that is independent of the loading type, geometry and boundary conditions, and depends only on the proximity of the crack. This fact allow the application of this technique in general composite material structures.

In figures 6,7 and 8, the wavelength shift and peak width at -30dBm, computed from the output of the FBG array in tree different loading conditions, is presented. Each different color plotted corresponds to each Bragg grating in the sensor array, being the FBG5 (Orange color line) the grating located closest to adhesive edge and the FBG1 (Black color line) the grating more distant. The crack growth in the order: FBG 5 $\rightarrow$ 4 $\rightarrow$ 3 $\rightarrow$ 2$\rightarrow$ 1.

The wavelength shift is dependent on the loading type, but the increase in the width of the peak is related to the presence of the crack (Birefringent effect and non-uniform strain). Using this information it is possible to track the crack by an abrupt variation of

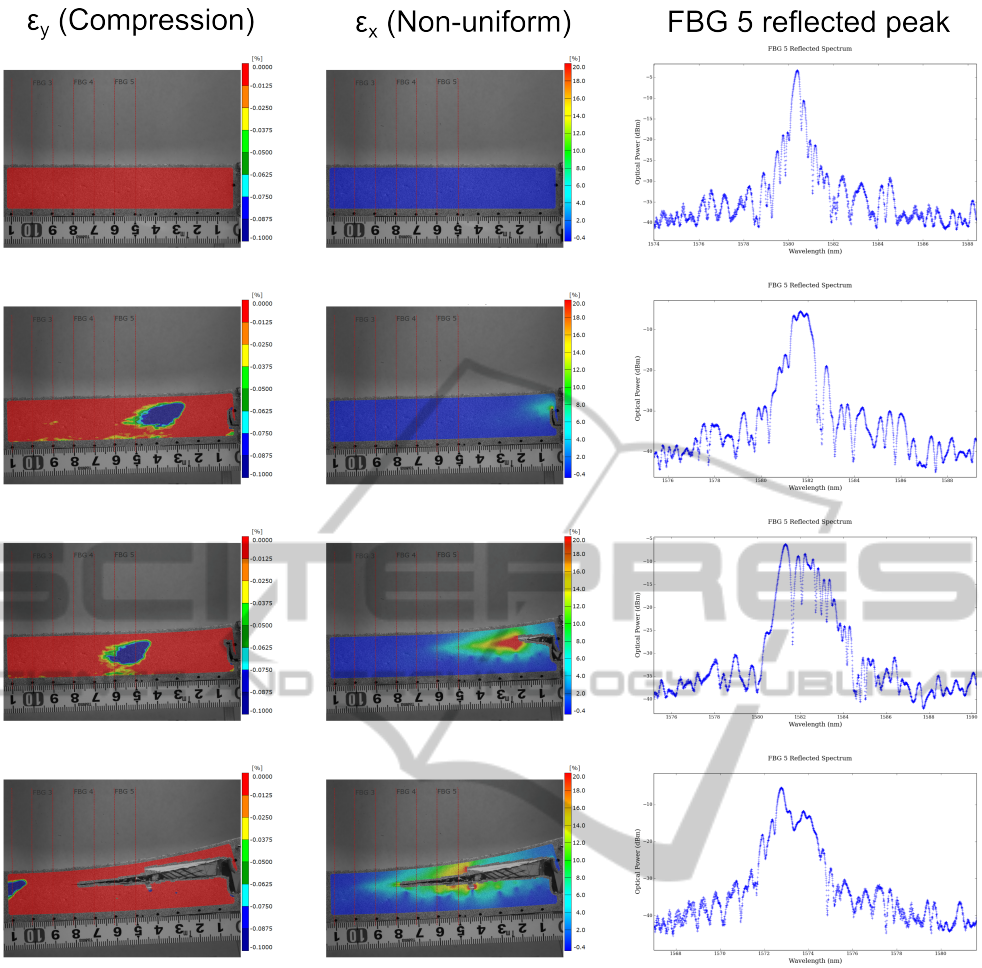

Figure 5: Different stages of the sensor output during a crack growth.

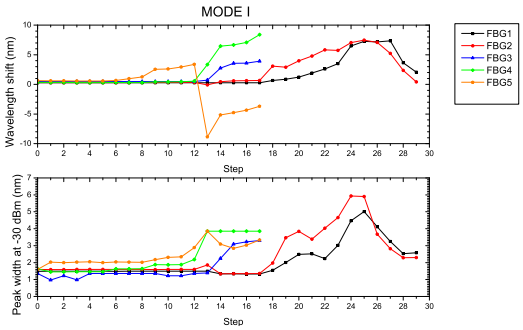

Figure 6: Sensor array output for Mode I crack growing.

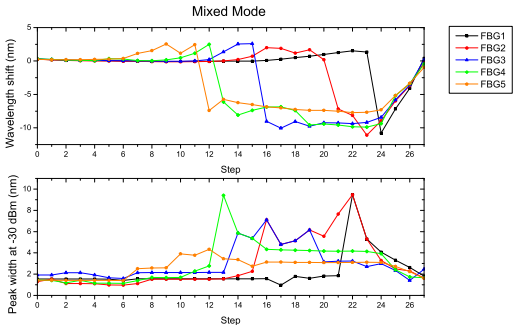

Figure 7: Sensor array output for Mixed Mode crack growing.

the wavelength and/or increase in the width of the reflected peak. This monitoring method can be implemented in a structural model using the equations developed in section 2. This makes it possible to study the application of this monitoring technique in other locations, predict the sensor output and determine the optimized sensor-structure configuration.

ACKNOWLEDGEMENTS

The authors acknowledges the Seventh Framework Programme (FP7) for funding the project MareWint (Project reference: 309395) as Marie-Curie Initial Training Network, Fibersensing for providing the

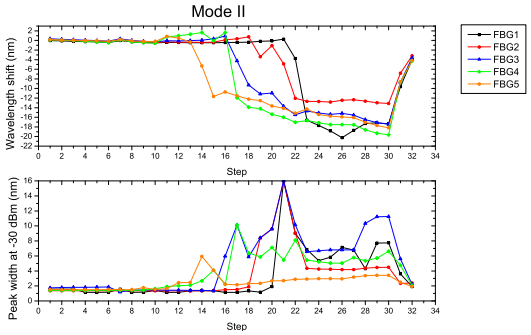

Figure 8: Sensor array output for Mode II crack growing.

FBG sensors and hardware, and SSP-Technology for providing the material tested.

REFERENCES

B.F. Sørensen, Technical Univ. of Denmark, R. N. L. f. S. E. M. R. D. (2010). *Cohesive laws for assessment of materials failure: Theory, experimental methods and application*. Risø DTU.

Bosia, F., Giaccari, P., Botsis, J., Facchini, M., and Limberger, H. (2003). Characterization of the response of fibre Bragg grating sensors subjected to a two-dimensional strain field. *Smart Materials and Structures*, 925(12):925–934.

Hill, K. and Meltz, G. (1997). Fiber Bragg grating technology fundamentals and overview. *Journal of lightwave technology*, 15(8):1263–1276.

Hu, H., B. Wang, C. L., and Su, J. (2006). Damage detection of surface cracks in composite laminates using modal analysis and strain energy method. *Composite Structures*, 74(4):399–405.

Jones, R. (1999). *Mechanics of composite materials*. Taylor & Francis.

Jülich, F. and Roths, J. (2010). Comparison of transverse load sensitivities of fibre Bragg gratings in different types of optical fibres. 7726(0):77261N–77261N–9.

Kyriazoglou, C. and Guild, F. (2004). Vibration damping for crack detection in composite laminates. *Composites Part A: Applied Science and Manufacturing*, 35(7-8):945–953.

Morey, W., Meltz, G., and Glenn, W. (1990). Fiber optic Bragg grating sensors. *OE/FIBERS'89*.

Peters, K., Studer, M., Botsis, J., Iocco, A., Limberger, H., and Salath, R. Embedded Optical Fiber Bragg Grating Sensor in a Nonuniform Strain Field : Measurements and Simulations. pages 19–28.

Silversides, I., Maslouhi, A., and Laplante, G. (2013). Interlaminar fracture characterization in composite materials by using acoustic emission 2 . Experimental procedures and FEM Modeling. (November):13–15.

Sørensen, B., Jørgensen, K., Jacobsen, T., and Østergaard, R. C. (2006). DCB-specimen loaded with uneven bending moments. *International Journal of Fracture*, 141(1-2):163–176.

Sørensen, L., Botsis, J., Gmür, T., and Cugnoni, J. (2007). Delamination detection and characterisation of bridging tractions using long FBG optical sensors. *Composites Part A: Applied Science and Manufacturing*, 38(10):2087–2096.

Yan, Y. and Yam, L. (2002). Online detection of crack damage in composite plates using embedded piezoelectric actuators/sensors and wavelet analysis. *Composite Structures*, 58(1):29–38.

Yashiro, S., Okabe, T., Toyama, N., and Takeda, N. (2007). Monitoring damage in holed CFRP laminates using embedded chirped FBG sensors. *International Journal of Solids and Structures*, 44(2):603–613.

Zhang, L., Zhang, W., and Bennion, I. (2008). *In-Fiber Grating Optic Sensor, Fiber Optic Sensors, Second Edition*. CRC Press.

Zhang, W., Chen, W., Shu, Y., Lei, X., and Liu, X. (2014). Effects of bonding layer on the available strain measuring range of fiber Bragg gratings. *Applied Optics*, 53(5):885.

Zhang, X., Max, J., and Jiang, X. (2007). Experimental investigation on optical spectral deformation of embedded FBG sensors. *SPIE, Photonics Packaging, Integration, and Interconnects VII*, 6478.